Journal of
Water & Climate Change

IWA PUBLISHING

Journal of Water and Climate Change Vol 15 No 7, 3377 doi: 10.2166/wcc.2024.260

Development of temperature and mass transfer-based empirical models for estimating reference evapotranspiration in Nigeria

Dauda Pius Awhari[a,b], Mohamad Hidayat Jamal[a,*], Mohd Khairul Idlan Muhammad[a], Matthew Boniface Kamai[b], Zaher Mundher Yaseen[c,d] and Shamsuddin Shahid[a,e]

[a] Department of Water and Environmental Engineering, Faculty of Civil Engineering, Universiti of Teknologi Malaysia (UTM), Johor Bahru 81310, Malaysia
[b] Department of Agricultural and Bioresources Engineering, Taraba State University, Jalingo, Nigeria
[c] Civil and Environmental Engineering Department, King Fahd University of Petroleum & Minerals, Dhahran 31261, Saudi Arabia
[d] Interdisciplinary Research Centre for Membranes and Water Security, King Fahd University of Petroleum & Minerals, Dhahran 31261, Saudi Arabia
[e] Environmental and Atmospheric Sciences Research Group, Scientific Research Center, Al-Ayen University, Thi-Qar, Nasiriyah, 64001, Iraq
*Corresponding author. E-mail: mhidayat@utm.my

ABSTRACT

The empirical models commonly employed as alternatives for estimating evapotranspiration provide constraints and yield inaccurate results when applied to Nigeria. This study aims to develop novel empirical models to enhance evapotranspiration (ET_0) estimation accuracy in Nigeria. The coefficients of non-linear equations were optimised using the particle swarm optimisation (PSO) algorithm for the development of the two new ET_0 models for Nigeria, Awhari1 (temperature-based) and Awhari2 (mass transfer-based). ERA5 reanalysis data with a $0.1° \times 0.1°$ resolution was used. The models were rigorously assessed against the FAO-56 Penman–Monteith method, resulting in Kling–Gupta efficiency (KGE) and percentage bias (Pbias) values of 0.75, 6.49, and 0.92, 5.67, respectively. The spatial distribution analysis of performance metrics showed both equations exhibited superior accuracy in estimating ET_0 across diverse climatic zones in Nigeria. The incorporation of PSO in model development, coupled with spatial analysis, highlights the study's multidimensional approach. The spatial performance of the models indicates that they can be valuable tools for water resource management, irrigation planning, and sustainable agriculture practices in Nigeria.

Key words: Awhari models, Nigeria, particle swam optimisation, Penman–Monteith

HIGHLIGHTS

- A novel spatial analysis evaluates the performance of the models across various climatic zones.
- Validation against FAO-56 confirms high model accuracy, as evidenced by high KGE and low bias values.
- The research provides valuable insights into water management and sustainable agriculture practices by incorporating PSO optimisation and spatial analysis.

GRAPHICAL ABSTRACT

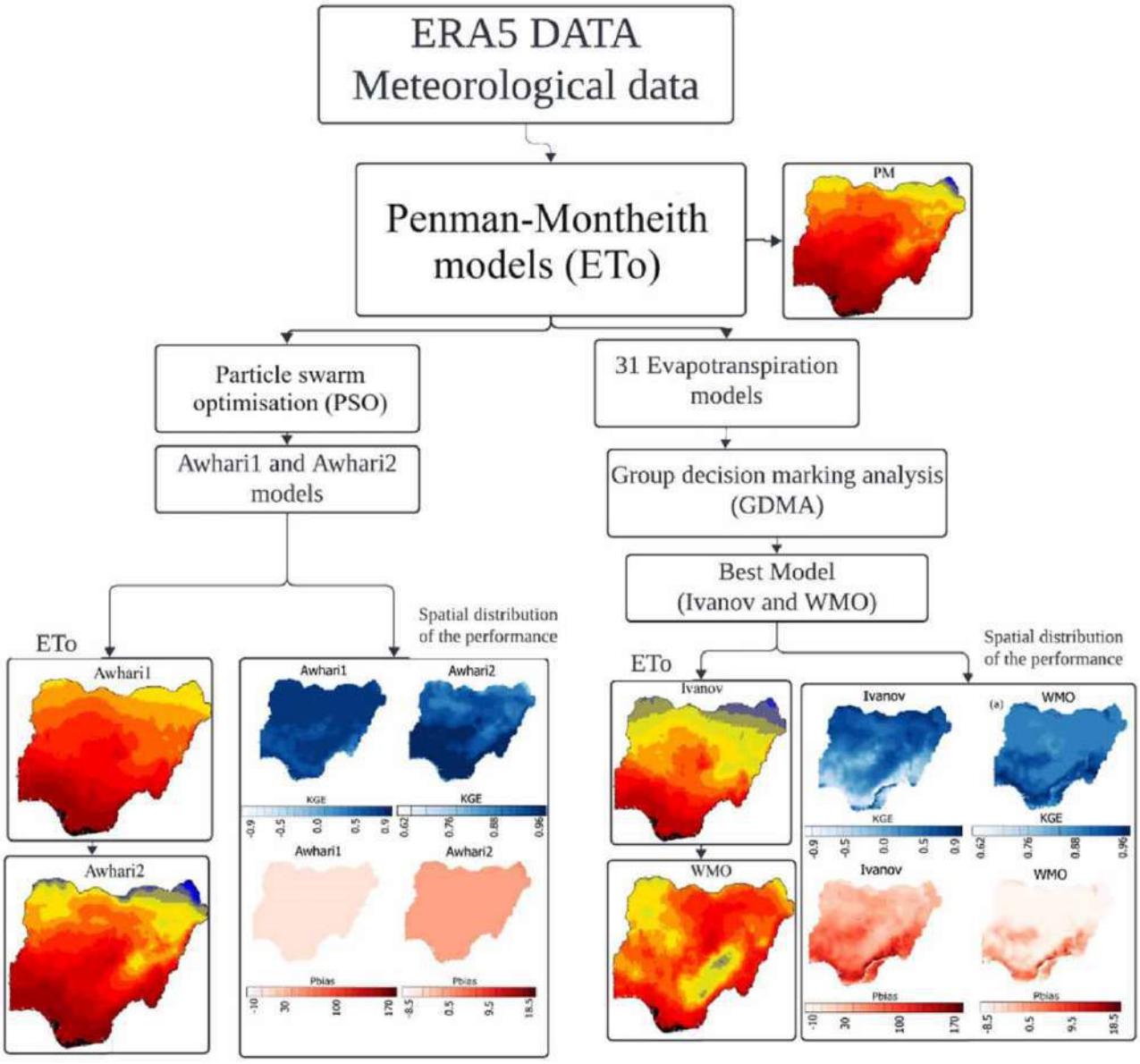

1. INTRODUCTION

Water is a precious resource, and efficient water management in agriculture is crucial for sustainable development in agricultural planning (García-Tejero *et al.* 2011; Zaman *et al.* 2017). Reference evapotranspiration (ET_0) is critical to understanding crops' water needs and planning effective irrigation strategies (Bai *et al.* 2017; Roy *et al.* 2021; Dong *et al.* 2024). ET_0 models serve as fundamental tools in irrigation and water resource management and represent the water requirement of well-watered reference crops, forming the basis for calculating crop water requirements and climate change. Accurate ET_0 estimation enables water resource managers to optimise irrigation scheduling, conserve water, and enhance agricultural productivity. In regions like Nigeria, where water management is a recurring challenge, precise ET_0 models are essential for sustainable water use.

Despite the global development of various empirical ET_0 models, none have been specifically tailored to the unique climatic conditions in Nigeria. This gap in the literature underscores the need for region-specific models that can account for the intricacies of Nigeria's diverse climate. Empirical models, which rely on observed data and are often more adaptable to local conditions, become paramount in addressing this gap and providing accurate ET_0 estimates for specific needs in Nigeria.

Many empirical models have been developed worldwide to estimate ET_0, often using readily available meteorological data, e.g., temperature, wind speed, and relative humidity (Trabert 1896; Meyer 1926; Linacre 1977; Ahooghalandari *et al.* 2016; Muhammad *et al.* 2022). While these models offer valuable tools, their accuracy can be significantly limited when applied in regions with unique climatic characteristics. Nigeria has a diverse landscape, ranging from humid coastal regions to arid northern savannas, each experiencing distinct rainfall patterns, wind speed, temperature regimes, and solar radiation profiles (Oguntunde *et al.* 2011; Shiru *et al.* 2020; Oloyede *et al.* 2022; Animashaun *et al.* 2023). This climatic heterogeneity challenges existing global ET_0 models, often leading to inaccurate estimates within the country.

The consequences of inaccurate ET_0 estimation can be substantial for irrigation, water resource management, and food security (Bashir *et al.* 2023; Awhari *et al.* 2024). Overestimating ET_0 can lead to excessive irrigation, wasting precious water resources, and potentially damaging soil through salinisation (Ankindawa & Awhari 2010; Al-Bakri *et al.* 2022). Conversely, underestimating ET_0 can cause water deficits, endanger crop yields, and contribute to food insecurity (Nikolaou *et al.* 2020). Therefore, developing dependable and region-specific ET_0 models for the Nigerian climate is crucial for optimising water management strategies and ensuring sustainable agricultural practices.

Numerous ET_0 models have been developed using temperature, solar radiation, wind speed, and various combinations to accurately predict evapotranspiration rates from surfaces such as soil, water, and vegetation canopies (Huang *et al.* 2021). The FAO-PM equation is widely recognised as the most effective approach for estimating ET_0 across various climatic conditions (Hernández-Bedolla *et al.* 2023; Wu *et al.* 2023). FAO-PM estimation is resource-intensive, and the necessary data are not readily accessible in underdeveloped countries like Nigeria. An inherent constraint in the widespread use of the universally recognised FAO-PM approach is the lack of access to the extensive data it requires at multiple meteorological stations, compounded by concerns over the quality of these data points.

This study aimed not to develop a novel approach that substitutes FAO-PM but to devise a straightforward method based on temperature and mass transfer-based models. This method relies solely on maximum temperature, wind speed, and relative humidity, making it suitable for areas where other climatic parameters are unavailable at the desired level of detail. The FAO-PM was used as the reference for formulating these novel methodologies. This research evaluated the model's effectiveness in accurately representing the spatial distribution of the performance metrics and compared it with FAO-PM as reference ET_0.

2. MATERIAL AND METHODS

2.1. Study area

Nigeria, situated in West Africa between latitudes 4°30′N and 14°30′N and longitudes 3°15′E and 14°45′E, boasts a geographical tapestry defined by diverse ecological zones. Benin bounds it to the west, Chad and Cameroon to the east, and Niger to the north, Nigeria's borders encompass a nation of varied topography, including plains, plateaus, and mountains, with an elevation of approximately 2,419 m, as shown in Figure 1. The ecological richness of Nigeria is manifested in distinct zones that significantly influence its climate and biodiversity. The southern rainforest zone features an abundance of vegetation and greenery in the rainforest region and high precipitation levels. In the central Savannah zone, including grasslands, wet and dry seasons facilitate agricultural activities. The northern Sahel zone presents semi-arid conditions with sparse vegetation, posing challenges for agriculture. Nigeria experiences a tropical climate, marked by a rainy season from April to October, notably in the rainforest and Savannah zones, and a dry season from November to March, affecting the entire nation. The harmattan, a dry and dusty trade wind, characterises the dry season, impacting visibility and lowering temperatures. Mean temperatures fluctuate across the country, with coastal areas having temperatures between 25 and 35 °C, while the northern interior may experience a range of 21–40 °C. Precipitation levels follow a similar pattern, with the southern regions receiving more rainfall, with average annual precipitation averages of 1,900 mm. The arid north receives an average scarce rainfall of around 400 mm. Daily air temperature, wind speed, and relative humidity data for 72 years (January 1950–December 2023) across Nigeria were retrieved from the ERA5 reanalysis dataset (0.1° × 0.1° resolution) (https://cds.climate.copernicus.eu/cdsapp#!/dataset/reanalysis-era5-land?tab=form) and were used to develop the models. Figure 2 illustrates the stepwise methodology for developing the temperature and mass transfer-based models.

2.2. Reference evapotranspiration equation

This study relied on the widely recognised FAO-PM model as the reference standard for ET_0 estimation. The accuracy of the FAO-PM models is widely accepted globally, and many researchers have used it as a reference in developing models and their suitability in different climate conditions (Ahooghalandari *et al.* 2016; Shiri 2017; Emeka *et al.* 2021). The FAO-PM model is

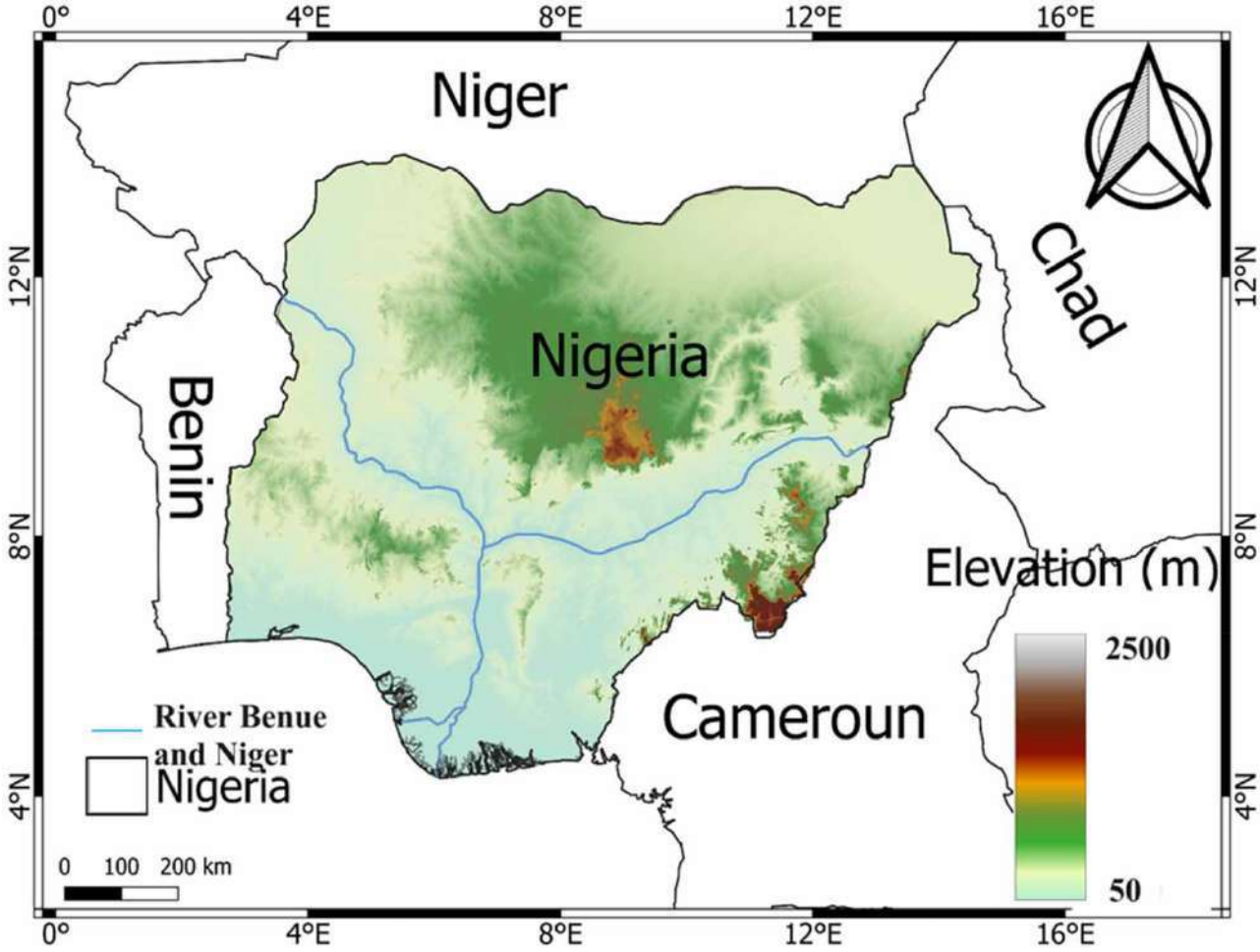

Figure 1 | The location of Nigeria and the spatial distribution of its elevation.

mathematically represented by the following equation:

$$ET_0 = \frac{0.408\Delta(R_n - G) + \gamma\left(\frac{900}{T+273}\right)u_2(e_s - e_a)}{\Delta + \gamma(1 + 0.34u_2)} \quad (1)$$

where Δ denotes the saturation vapour pressure curve gradient in kPa/°C. R_n refers to the net radiation in mm/day. G represents the density of soil heat flow (mm/day), and T_a is the mean air temperature (°C). The variable 'e_a' represents the current vapour pressure in kPa, whereas 'e_s' represents the saturation vapour pressure in kPa. The variable 'u_2' represents the wind speed (m/s) at a height of 2 m, which is derived using the 'u_{10}' data via the wind profile relationship. The psychrometric constant γ is measured in kPa/°C, the surface resistance rs is measured in s/m, and the latent heat of vaporisation λ is measured in MJ/kg.

This study first assessed 31 empirical models, as shown in Table 1, consisting of 20 models based on temperature and 11 models based on mass transfer. Kling–Gupta efficiency (KGE) (Gupta & Kling 2011) and percentage bias (Pbias) were used for this purpose. KGE measures correlation, variability ratio, and mean bias between two datasets and is considered a better metric for assessing model performance. Pbias provides the mean bias in ET_0 estimation and thus serves as a simple measure of model deviation from the observation.

Ivanov and World Meteorological Organization (WMO) performed better among these models based on their KGE values, as shown in Table 1. These models were the main focus of our investigation. A novel temperature technique that utilises

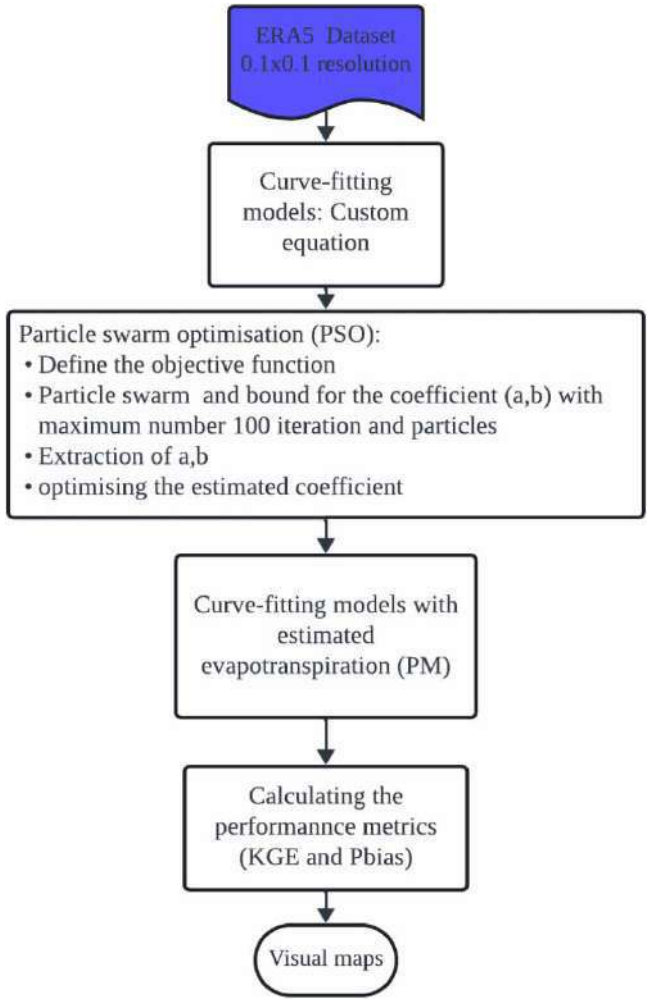

Figure 2 | Step-by-step methodology flowchart of the study.

maximum temperature and relative humidity to determine ET_0 was derived. Ivanov generally performs accurately across the specified region among the temperature-based models. There is a need to build a straightforward temperature approach that can effectively work at all locations throughout the nation. As a result, a novel empirical temperature equation using maximum temperature and relative humidity was developed. In developing a new technique, the aerodynamic term was calculated based on the mean vapour pressure deficit (Dav). It is suggested that Dav may be estimated as 1 – RH/100, where RH represents the relative humidity. ET_0 is closely associated with extra-terrestrial radiation (Ahooghalandari *et al.* 2016). The new equations were derived by integrating the expression (1 – RH/100) with the maximum temperature.

The mass transfer method is one of the oldest and simplest methods because of its reasonable evaporation accuracy (Singh & Xu 1997; El-Mahdy *et al.* 2021). The mass transfer-based models are built around the concept of Dalton's equation, which is the free water surface and is expressed as follows:

$$ET_0 = C(e_s - e_a) \tag{2}$$

ET_0 represents the evaporation of water from the free surface, e_s represents the saturated vapour pressure at the water surface temperature, e_a represents the vapour pressure in the air, and C represents the aerodynamic conductivity (Singh & Xu 1997), which is influenced by factors, such as horizontal wind speed, surface roughness, and thermally generated turbulence, as presented in the following equation:

$$ET = f(u)(e_s - e_a) \tag{3}$$

Table 1 | Reference evapotranspiration model methods

No.	Model	Inputs	Equation	KGE	Pbias	References
Temperature-based models						
1	Linacre	T	$\mathrm{ET}_0 = \dfrac{\frac{700(T \pm 0.006z)}{100 - L} + 15(T - T_\mathrm{d})}{80 - T}$	0.092	61.0	Linacre (1977)
2	Hamon	T	$\mathrm{ET}_0 = 0.165 L_\mathrm{d} \mathrm{RHOSAT} \times \mathrm{KPEC}$	−47.00	−89.4	Hamon (1963)
3	FAO-Blaney	T	$\mathrm{ET}_0 = p(0.46T + 8.13)$	−5,199.18	−11,031.0	Dooreng & Pruitt (1977)
4	Kharrufa	T	$\mathrm{ET}_0 = 0.34pT^{1.3}$	−0.48	86.6	Kharrufa (1985)
5	Ahooghalandari-1	T, RH	$\mathrm{ET}_0 = 0.252\left(\frac{R_\mathrm{a}}{\gamma}\right) + 0.221T_\mathrm{mean}\left(1 - \frac{\mathrm{RH}_\mathrm{mean}}{100}\right)$	0.001	61.5	Ahooghalandari *et al.* (2016)
6	Ahooghalandari-2	T, RH	$\mathrm{ET}_0 = 0.29\left(\frac{R_\mathrm{a}}{\gamma}\right) + 0.15T_\mathrm{max}\left(1 - \frac{\mathrm{RH}_\mathrm{mean}}{100}\right)$	−0.10	68.1	Ahooghalandari *et al.* (2016)
7	Ivanov	T, RH	$\mathrm{ET}_0 = 0.00006(25 + T)^2(100 - \mathrm{RH})$	0.33	54.2	Romanenko (1961)
8	Papadakis	T, RH	$\mathrm{ET}_0 = 2.5(e_{ma} - e_\mathrm{a})$	0.19	73.8	Papadakis (1965)
9	Hargreaves – Samani	T, T_max, T_min, R_a	$\mathrm{ET}_0 = (0.0023)*\sqrt{T_\mathrm{max} + T_\mathrm{min}}(T + 17.8)*R_\mathrm{a}$	-4.30×10^6	-9.20×10^6	Hargreaves & Samani (1985)
10	Baier-Robertson	T, T_max, T_min, R_a	$\mathrm{ET}_0 = 0.109\left(\frac{R_\mathrm{a}}{\lambda}\right) + 0.157*T_\mathrm{max} + 0.158\ (T_\mathrm{max} - T_\mathrm{min})$	−537.1	−1,072.7	Baier & Robert (1965)
11	Modified Baier	T, T_max, T_min, R_a, RH	$\mathrm{ET}_0 = 0.1844(T_\mathrm{max} - T_\mathrm{min}) + 0.1136R_\mathrm{a}(e_\mathrm{s} - e_\mathrm{a}) - 0.0039T_\mathrm{max} - 4.04$	8.77×10^5	1.93×10^6	Baier (1971)
12	Modified H-S1	T, T_max, T_min, R_a	$\mathrm{ET}_0 = 0.408*0.003*(T + 20)\mathrm{TD}^{0.4}R_\mathrm{a}$	1.14×10^6	-2.45×10^6	Droogers & Allen (2002)
13	Modified H-S2	T, T_max, T_min, R_a	$\mathrm{ET}_0 = 0.408*0.0025*(T + 16.8)\mathrm{TD}^{0.5}R_\mathrm{a}$	-4.67×10^5	1×10^8	Droogers & Allen (2002)
14	Trajkovic	T, T_max, T_min, R_a	$\mathrm{ET}_0 = (0.0023R_\mathrm{a})\mathrm{TD}^{0.424}(T + 17.8)$	−371.43	−813.5	Trajkovic (2007)
15	Ravazzani	T, T_max, T_min, R_a	$\mathrm{ET}_0 = (0.817 + 0.00023R_\mathrm{a})(\mathrm{TD}^{0.5})(T + 17.8)$	-9.39×10^7	-2.01×10^7	Ravazzani *et al.* (2012)
16	Schendel	T, RH	$\mathrm{ET}_0 = 16\left(\frac{T}{\mathrm{RH}}\right)$	−1.64	163.7	Schendel (1967)
17	Dorji	T, T_max, T_min, R_a	$\mathrm{ET}_0 = 0.002*0.408R_\mathrm{a}(T + 33.9)(T_\mathrm{max} - T_\mathrm{min})^{0.296}$	−332.22	−695.8	Dorji *et al.* (2016)
18	Berti	T, T_max, T_min, R_a	$\mathrm{ET}_0 = 0.00193R_\mathrm{a}(T + 17.8)(T_\mathrm{max} - T_\mathrm{min})^{0.517}$	−1,031.3	−2,259.8	Berti *et al.* (2014))
19	Talee and Tabari	T, T_max, T_min, R	$\mathrm{ET}_0 = [0.0031*R_\mathrm{a}(T + 17.8)(T_\mathrm{max} - T_\mathrm{min})^{0.5}]/\lambda$	−1,817.3	−2,706.3	Tabari & Talaee (2011)
20	Drogers and Allen	T, T_max, T_min, R	$\mathrm{ET}_0 = [0.003*R_\mathrm{a}(T + 20)(T_\mathrm{max} - T_\mathrm{min})^{0.4}]/\lambda$	−1,336.9	−2,903.2	Droogers & Allen (2002)
Mass transfer-based models						
21	Mahringer	T, RH, u	$\mathrm{ET}_0 = (0.\ 15072)\sqrt{3.6u}(e_\mathrm{s} - e_\mathrm{a})$	0.74	18.96	Mahringer (1970)

(*Continued.*)

Table 1 | Continued

No.	Model	Inputs	Equation	KGE	Pbias	References
22	Penman	T, RH, u	$\mathrm{ET}_0 = \left(2.625 + \frac{0.000479}{u}\right)(e_s - e_a)$	0.72	−10.17	Penman (1948)
23	Rohwer-2	T, RH, u	$\mathrm{ET}_0 = (3.3 + 0.891(u))(e_s - e_a)$	0.20	59.62	Rohwer (1931)
24	Szasz	T, RH, u	$\mathrm{ET}_0 = 0.00536(T+21)^2\left(1 - \frac{\mathrm{RH}}{100}\right)^{\frac{2}{3}} f(u)$ $f(u) = (0.0519u) + 0.905$	0.37	55.16	Szasz (1973)
25	Trabert	T, RH, u	$\mathrm{ET}_0 = (0.3075)\sqrt{u}(e_s - e_a)$	0.62	27.92	Trabert (1896)
26	WMO	RH, u	$\mathrm{ET}_0 = 0.1298 + 0.0934(u)(e_s - e_a)$	0.89	6.63	WMO *et al.* (1966)
27	Albrecht	T, RH, u	$\mathrm{ET}_0 = 0.1005 + 0.297(u)(e_s - e_a)$	−0.33	90.10	Albrecht (1950)
28	Meyer	T, RH, u	$\mathrm{ET}_0 = (0.375 + 0.05026(u))(e_s - e_a)$	0.28	54.67	Meyer (1926)
29	Brockamp–Wenner	T, RH, u	$\mathrm{ET}_0 = 0.543(u^{0.456})(e_s - e_a)$	−0.69	121.70	Brockamp & Wenner (1963)
30	Fitzgerald	T, RH, u	$\mathrm{ET}_0 = 0.44 + 0.19u\ (e_s - e_a)$	-3.62×10^5	7.69×10^5	FitzGerald (1886)
31	Saif	RH, u	$\mathrm{ET}_0 = (0.37 + 0.72u)(e_s - e_a)$	-6.38×10^5	1.34×10^6	Islam *et al.* (2020)

Note: ET_0 is the reference evapotranspiration (mm/day), ND is the length of time interval (day), and f is a correction factor that varies with the average annual temperature ($T_a < 23.5$ °C, $F = 0.01$). R_a is the extra-terrestrial radiation (MJ/m^2/day), u is the wind speed at 2 m (m/s), RH is the relative humidity (%), T, T_{max}, T_{min} are average, maximum, and minimum air temperature (°C), T_d is the daily dewpoint air temperature in (°C), TD is the difference between the T_{max} and T_{min} (°C), e_{ma} is the saturation vapour pressure at the monthly mean daily maximum temperature (kPa), and e_a and e_s represent actual and saturation vapour pressure (kPa), except for Penman, Papadakis, and Rohwer (kPa), RHOSAT is the saturated vapour density (g/m^3), KPEC is a calibration coefficient (1.2), p is a constant having two values (0.27 and 0.28), $f(u)$ denotes a function of wind speed, L is the latitude at each point (degree), z is the elevation (m), λ represents latent heat of evaporation (MJ/kg), Δ is the slope of saturation vapour pressure–temperature curve (kPa/°C), and γ is the psychometric constant (kPa/°C).

where $f(u)$ represents the wind function, which depends on observation heights, wind, and vapour pressure. This study developed a new, simple empirical mass transfer model based on established principles and techniques.

2.3. Models development

The two models, Awhari1 (temperature-based) and Awhari2 (mass transfer-based), were developed through curve-fitting techniques and particle swarm optimisation (PSO). These equations evaluate the fitness function for ET_0 estimation, incorporating varying '*a*' and '*b*' values and discrepancies between simulated and observed ET_0 values. To optimise model performance, we implemented PSO, a technique that iteratively refines the objective function for each particle. This involves the concurrent execution of both the ET_0 model and the simulated evapotranspiration model, with dynamic adjustments to each particle's velocity and position based on historical best positions and those discovered within the swarm. The optimised models, identified through personal and global best positions, underwent rigorous evaluation by comparing simulated and observed ET_0. The two constants, a and b, were set with options and bounds for coefficients [a, b], lb = lower bounds for coefficients [a, b], ub = upper bounds for coefficients, and max iterations of 100. The two constant values for the temperature and mass transfer-based models, a and b, were calculated using PSO over the years 1950–2022.

2.3. Theory of PSO

The PSO is a metaheuristic optimisation algorithm inspired by the social behaviour of birds flocking or fish schooling. PSO aims to iteratively improve a population of potential solutions by simulating the behaviour of particles in a multidimensional search space. The following are the steps, as illustrated in Figure 3.

i. *Initialisation*: The PSO algorithm begins by creating a swarm of particles in a defined search space. Each particle represents a potential solution to the optimisation problem, equipped with randomly assigned positions and velocities.

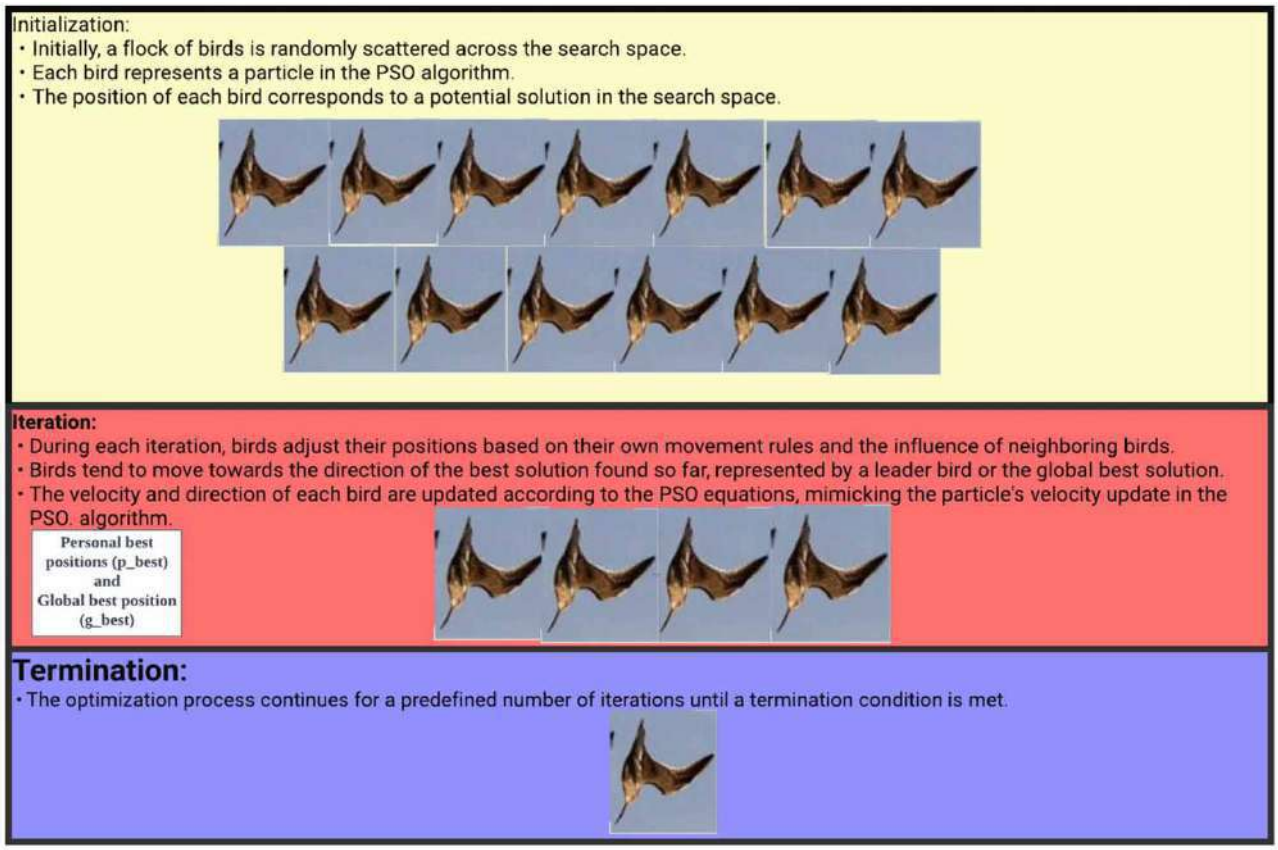

Figure 3 | Illustration of the PSO technique.

ii. *Fitness evaluation*: The performance of each particle is evaluated using a predefined fitness function that quantifies how well its position conforms to the optimal solution. This feature is key in guiding the search towards the desired regions.
iii. *Velocity update*: Particle movement is influenced by three key factors:

- *Inertia*: This component encourages continued exploration by maintaining momentum in the current direction.
- *Cognitive component*: Each particle remembers its best-known position (personal best) and is drawn towards it, promoting the exploitation of previously identified promising areas.
- *Social component*: Particles also possess an awareness of the swarm's best position (global best) and are attracted towards it, facilitating exploration of promising regions identified by others.

iv. *Position update*: Based on their updated velocities, particles move within the search space, effectively exploring neighbouring regions.
v. *Personal and global best update*: Upon reaching their new positions, particles compare them to their respective personal best positions. If an improvement is found, the personal best is updated. The global best position is also constantly tracked and updated if any particle discovers a superior solution.
vi. *Termination*: The iterative process continues until a predefined termination criterion is met. This could include reaching a maximum number of iterations, achieving a satisfactory solution quality, or exhausting a set computational budget.
vii. *Final solution*: The best-known position discovered by any particle in the swarm represents the optimal or near-optimal solution to the optimisation problem.

3. RESULTS

3.1. Development of Awhari1 and Awhari2 models

The model development using PSO involved optimising the coefficients of two non-linear equations using termination criteria based on temperature and mass transfer models. The equations optimised to develop the new models are:

$$\mathrm{ET}_0 = a(1 - b\mathrm{RH})T_{\max} \tag{4}$$

$$\mathrm{ET}_0 = a + b(u)(e_s - e_a) \tag{5}$$

where a and b are the coefficients optimised with u, e_s, e_a, RH, and $T_{\max}$. Equation (4) is a temperature-based model, and Equation (5) is a mass transfer-based model. The PSO algorithm finds optimal values of a and b to fit the observed data. The PSO algorithm was executed for 100 iterations with predefined lower and upper bounds to optimise the coefficients a and b. During the evolution process, the PSO algorithm iteratively updated the positions of particles in the search space, aiming to minimise or maximise the objective function (Kohler *et al.* 2019; Gad 2022), which is KGE between the model simulated and observed ET_0. The PSO algorithm iteratively adjusted the coefficients a and b for each equation within the specified bounds, optimising them to fit the data best. The termination criteria guided the algorithm to stop once satisfactory convergence was achieved. This ensures that the algorithm terminates when further iterations are unlikely to improve the solutions significantly. The process produces two equations:

$$\text{Awhari1: } \mathrm{ET}_0 = 0.3648\ (1 - 0.0104\mathrm{RH})T_{\max} \tag{6}$$

$$\text{Awhari2: } \mathrm{ET}_0 = 0.6337 + 1.6018(u)(e_s - e_a) \tag{7}$$

Equation (6) is a temperature-based model termed as 'Awhari1' and Equation (7) is the mass transfer-based model termed as 'Awhari2'.

3.2. Models performance

3.2.1. Temperature-based Awhari1 model

Figure 4(a)–4(c) depicts the spatial distribution of the ET_0 estimated using the Awhari1, Ivanov, and FAO-PM models. The figures reveal that the Awhari1 model (Figure 4(c)) could accurately replicate the spatial patterns of ET_0 values exhibited by the FAO-PM models, outperforming the Ivanov model (Figure 4(b)). The ET_0 estimated by Awhari1 and PM ranged between 0 and 10 mm/day, except in the Lake Chad basin, where FAO-PM estimated ET_0 had 11–13 mm/day. The Ivanov had higher ET_0 in the northern part, with range values of 6–14 mm/day and a higher ET_0 of 14 mm/day at the Lake Chad basin.

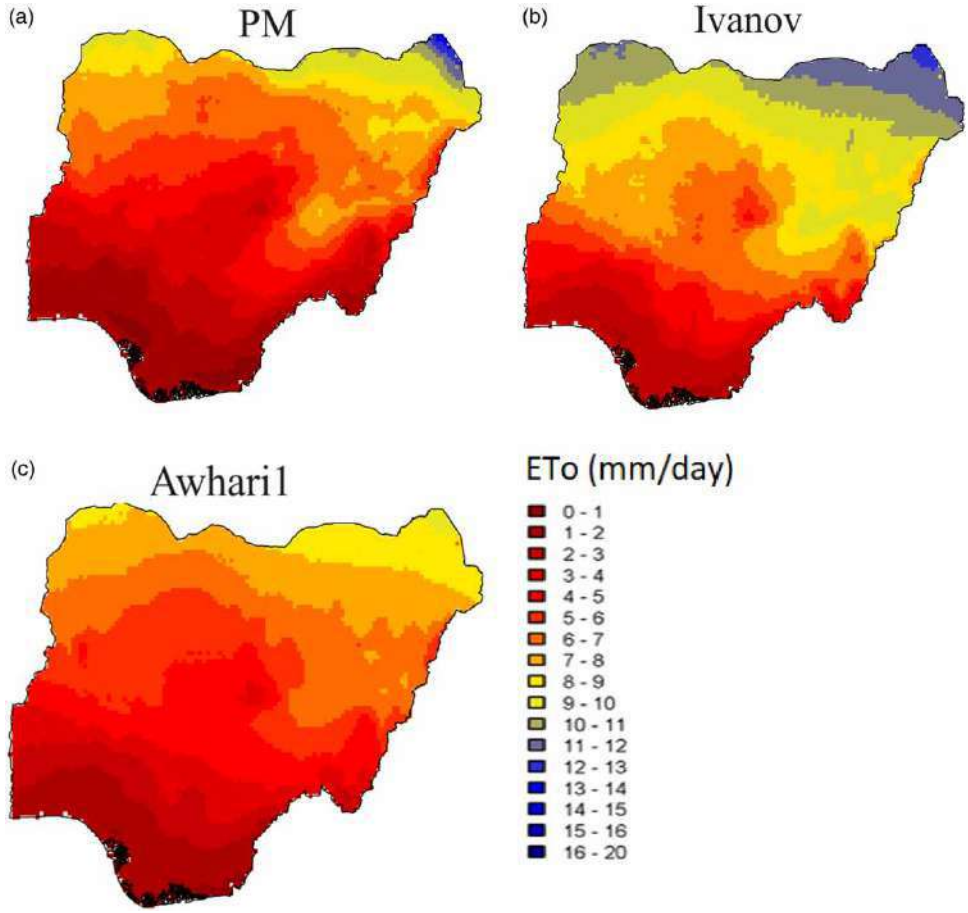

Figure 4 | Spatial distribution of ET_0 (mm/day) estimated using (a) PM, (b) Ivanov, and (c) Awhari1 model.

Figure 5 shows the spatial distribution of KGE and Pbias values for the Ivanov and newly developed Awhari1 models compared with the FAO-56 PM models across all grid cells. Ivanov's KGE ranges from −1.65 to 0.75 with a mean of 0.33, while its Pbias ranges from −6.30 to 205.89 with a mean of 54.20 in Table 2. Awhari1 showed KGE ranging from −0.26 to 0.89 with a mean of 0.75 and Pbias between 0.47 and 1.82 with a mean of 0.48. This excellent performance by the new models is evident in 98% of the grid cells, surpassing the Ivanov model, which only performs well in the northern region.

The boxplots of daily ET_0 estimated by the Awhari1, Ivanov, and FAO-56 PM models in the study area are shown in Figure 6(a). Similarly, the new model provided the ET_0 distribution most similar to the PM model, with a median value of 4.6 mm/day, while Ivanov has 5.2 mm/day.

The probability density function (PDF) of the estimated ET_0 using Awhari1, Ivanov, and PM models for the whole study region is shown in Figure 6(b). PM and Awhari1 showed peak densities, ET_0 of 0.18 and 2.3 mm/day, and median ET_0 values of 4.6 mm/day, respectively. Compared with the PM ET_0, Ivanov exhibits a lower peak density of 0.14 and a slightly lower median ET_0 of 4.4 mm/day, suggesting a tendency to underestimate ET_0. The tail behaviour of PM ET_0 towards tails gradually fades towards zero, reflecting the decreasing probability of extreme ET_0 values and the Awharil1 model. The shorter left tail implies a lower probability of underestimating extreme ET_0 events. The Ivanov model's longer right tail suggests a higher chance of overestimating extreme ET_0 events.

3.2.2. Mass transfer-based Awhari2 model

Figure 7(a)–7(c) presents a spatial distribution of potential evapotranspiration (PET) estimates across the grid cell. Awhari2 and PM estimated ET_0 ranged between 0 and 10 mm/day across all grid cells, except for the Lake Chad basin, where the WMO and Awhari2 exhibit slightly higher ET_0 (11–13 mm/day). Notably, the WMO displays a greater spatial variation in ET_0, reaching a maximum of 11 mm/day in the northwestern and Benue basins.

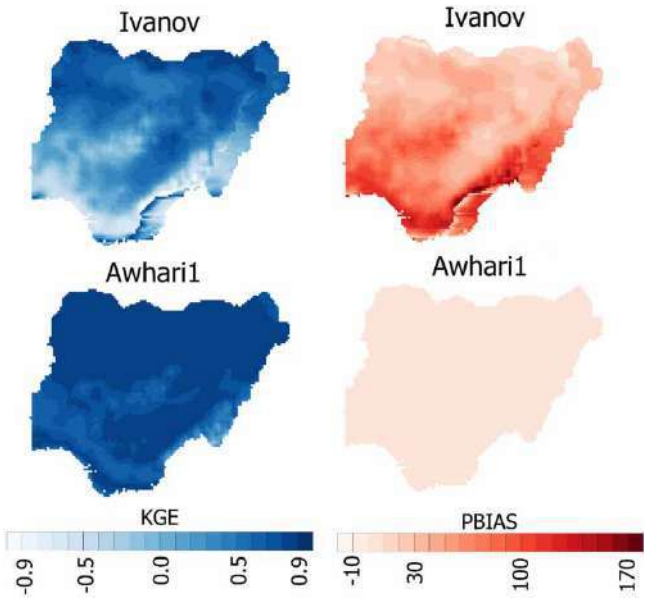

Figure 5 | Spatial distribution of KGE and Pbias % of the Ivanov and Awhari1 methods in estimating ET_0.

Table 2 | Statistical performance of the models against the FAO-PM model in estimating daily ET_0

S/No	Performance metrics	Ivanov	WMO	Awhari1	Awhari2
1	Pbias	54.20	−6.63	0.48	5.67
2	KGE	0.33	0.89	0.75	0.93

Figure 8 shows the spatial distribution of KGE and Pbias for the WMO and Awhari2 models compared with the FAO-56 PM model. WMO shows KGE ranging from 0.65 to 0.92 (mean 0.89) and Pbias ranging from −11.12 to 20.90 (mean −6.63). Awhari2 exhibits better performance, with KGE ranging from 0.76 to 0.99 (mean 0.92) and Pbias between 0.010 and 0.95 (mean 5.67) in Table 2. The Awhari2 model performed excellently in all the grid cells, with absolute performance in the southern part of the country. KGE values are not less than 0.95 in the region.

The boxplots of daily ET_0 estimated by the Awhari2, WMO, and PM models are shown in Figure 9(a). The Awhari2 model provided the most similar ET_0 distribution as the PM model, with a median value of 4.6 mm/day, while WMO underestimated ET_0 by 4.4 mm/day.

The PDF of the ET_0 estimated using PM, WMO, and Awhari2 models for the whole study region is shown in Figure 9(b). PM and Awhari2 peaked at 0.17 and 0.16 and ET_0 of 2.6 mm/day and median values of 4.6 mm/day for both the PM and the models. WMO exhibits a higher peak density at 0.2. The tail behaviour of the Awharil2 model's longer left tail implies a higher probability of overestimating extreme ET_0 events. The WMO model's shorter right tail suggests a higher chance of underestimating extreme ET_0 events.

4. DISCUSSION

The present study developed empirical PSO models for reliable ET_0 estimation using the ERA5 reanalysis temperature, wind speed, and relative humidity data. Several studies have endorsed the use of ERA5 reanalysis data for investigating the climate of West Africa (Quagraine *et al.* 2020; Steinkopf & Engelbrecht 2022; Bodjrenou *et al.* 2023; Gbode *et al.* 2023). Compared with its predecessor, ERA-Interim, ERA5 notably improves in representing various climatic aspects. Quagraine *et al.* (2020) demonstrated that ERA5 provides a more accurate depiction of precipitation patterns across West Africa, particularly by capturing crucial interannual variability and regional variations in summer monsoon rainfall. ERA5 also shows reduced biases in the annual cycle, resulting in a more precise representation of seasonal temperature fluctuations (Gbode *et al.* 2023). In

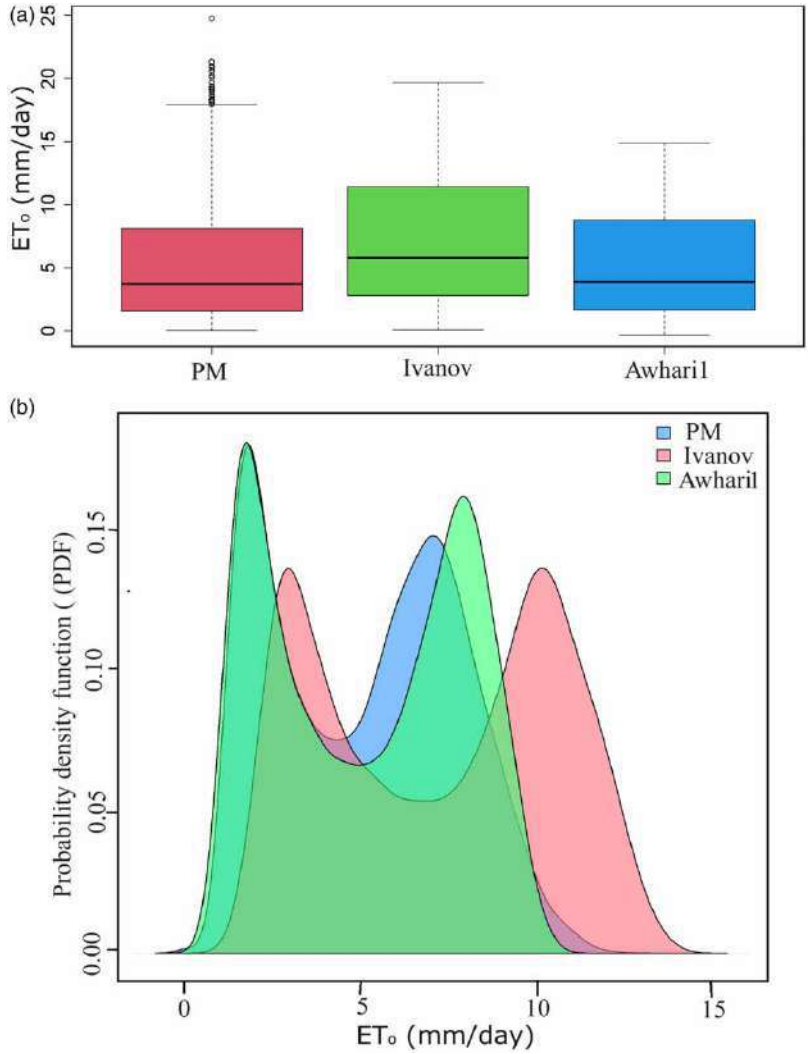

Figure 6 | (a) Boxplot of the ET_0 (mm/day) estimated using PM, Ivanov, and Awhari1 models, (b) probability distribution function of the ET_0 estimated using PM, Ivanov, and Awhari1 models.

addition, ERA5 exhibits improved capabilities in capturing interannual temperature variations (Bodjrenou *et al.* 2023). ERA5 data have also been found suitable for agricultural study (Araghi *et al.* 2022). Therefore, the results obtained in this study using ERA5 reanalysis climate data can be considered reliable.

The comparison of the newly developed models showed higher performance in terms of the statistical indices KGE and Pbias compared with the existing widely used models. The performance of the models showed considerable and promising improvement. For example, the newly developed temperature-based Awhari1 shows a mean KGE of 075 and Pbias of 6.49% compared with the Ivanov with KGE values of 0.33 and Pbias of 54.20%. In contrast, the WMO shows KGE values of 0.89 and Pbias of −6.63, and Awhari2 exhibits even better performance with KGE values of 0.92 and Pbias of 5.67%. This indicates a significant improvement in both the KGE and Pbias and the capability of newly developed models to estimate ET_0 in Nigeria with higher accuracy and less uncertainty. The spatial variability of a model's parameter development is significant because it provides an inside look at all the grid points where a model can be calibrated and validated to know it, thereby addressing the daily percentage bias varies in design irrigation and water resource management for crop production. The striking comparison that can be made on the performance of an equation can be seen from the spatial point of the observed and computed daily evaporation. This study brings an insight into the spatial performance of models that can easily be identified where the Pbias of the models developed can be addressed between the observed values across the grid cell and adjusted

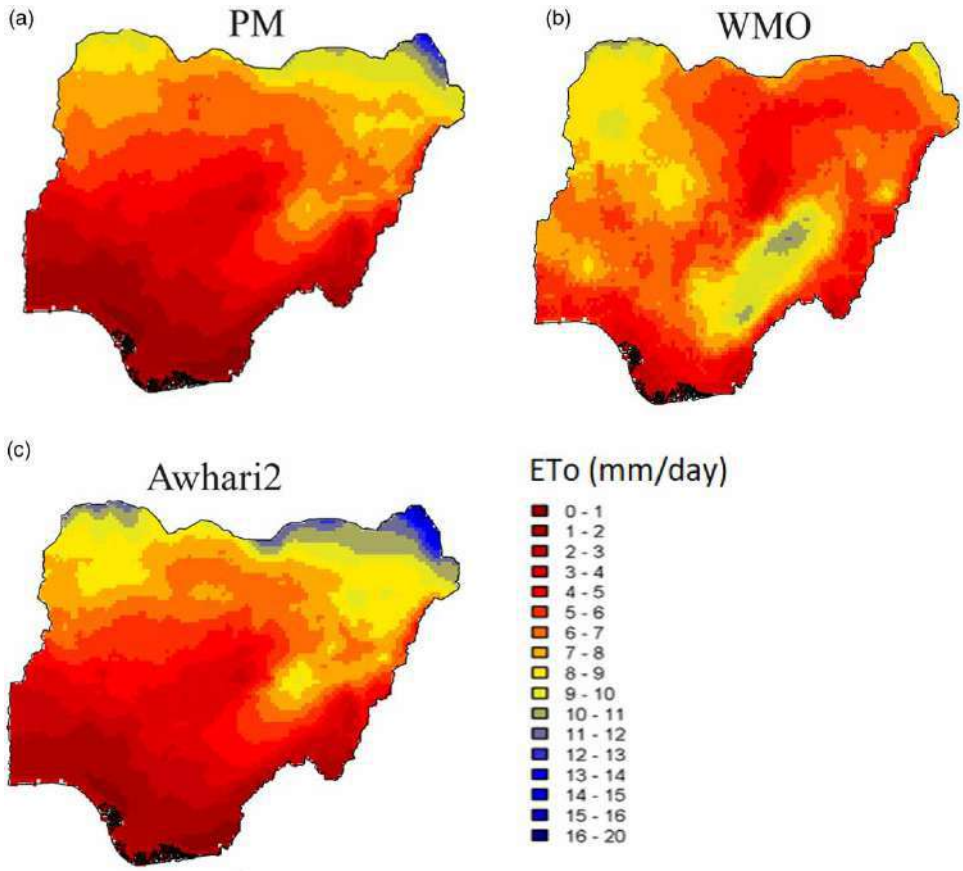

Figure 7 | Spatial distribution of ET_0 (mm/day) estimated using (a) PM, (b) WMO, and (c) Awhari2 model.

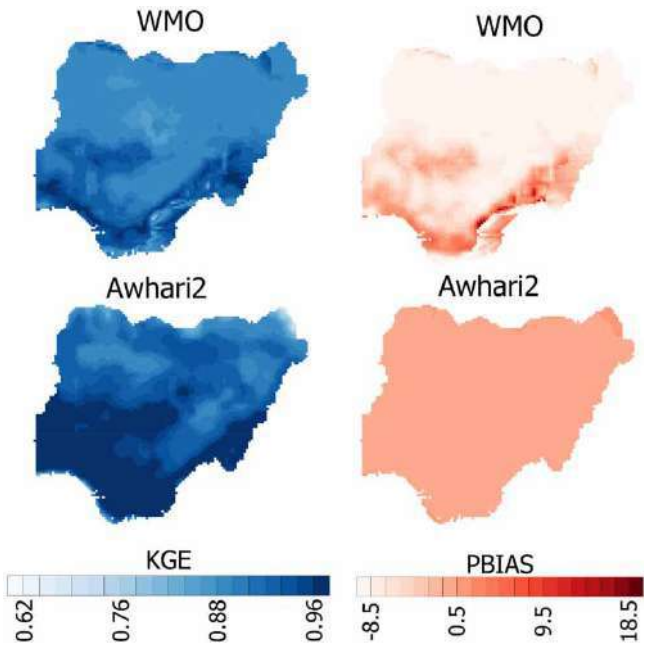

Figure 8 | Spatial distribution of KGE and Pbias % of WMO and Awhari2 in estimating ET_0.

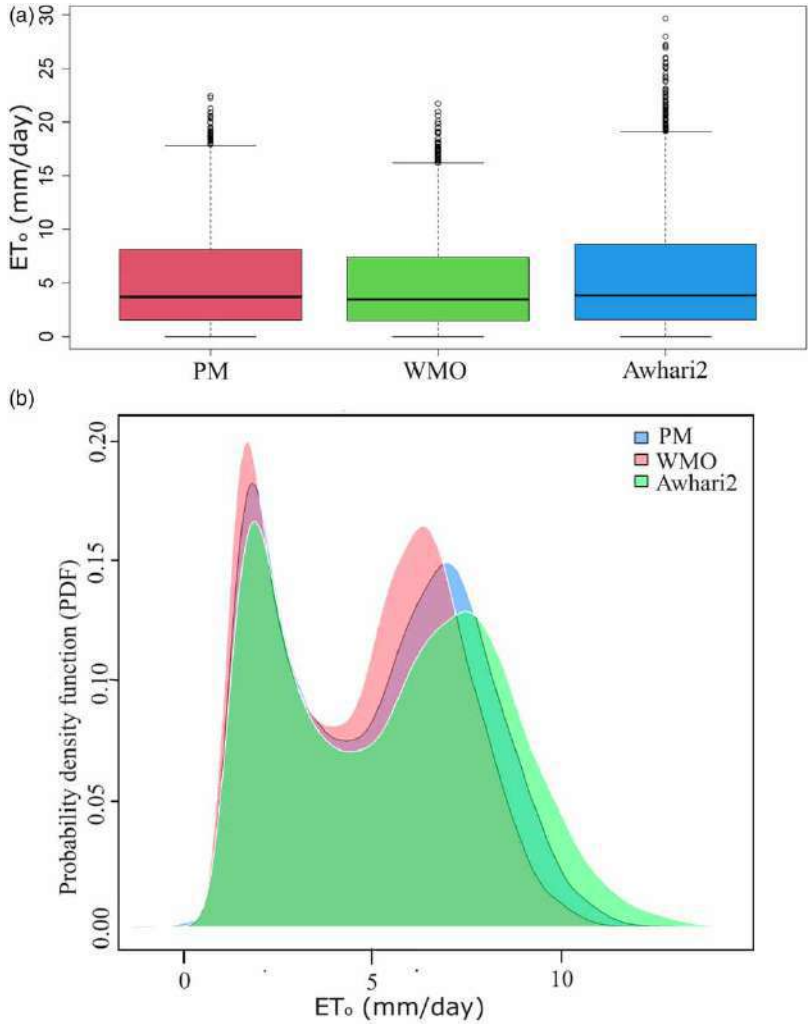

Figure 9 | (a) Boxplot of the ET_0 (mm/day) estimated using PM, WMO, and Awhari2 models, (b) probability distribution function (PDF) of the ET_0 estimated using PM, WMO, and Awhari2 models.

to the required values. This means that an acceptance level of confidence can be achieved when transferring the model's applicability from one region to another, even within a large region.

PSO is a potent and adaptable optimisation technique because of its global search powers, resilience, and ease of implementation (Juneja & Nagar 2016; Wang *et al.* 2018). It is a viable solution for many optimisation issues because of its unique properties, despite its strengths and shortcomings. It efficiently navigates the search space, avoiding being trapped in local optima (Gad 2022; Zhang & Kong 2023). This is accomplished by the swarm intelligence process, in which particles exchange information and draw insights from one another's achievements, thus avoiding premature settling on less-than-ideal solutions. PSO tolerates noise and complicated search landscapes, making it appropriate for situations with non-smooth objective functions or noisy data. It may be easily adjusted for different optimisation issues by parameter modifications or the inclusion of other processes. PSO is more computationally efficient than other population-based algorithms (Xu *et al.* 2023; Zhang & Kong 2023). Furthermore, PSO promotes information exchange among particles, accelerating algorithmic convergence. Population-based approaches are effective for smooth objective functions with well-defined gradients but may be susceptible to local optima and struggle with noisy functions. In contrast, PSO is more resilient (Gad 2022). This advantage has contributed to the development of superior ET_0 models.

Developing innovative evapotranspiration models in Nigeria might significantly impact agriculture, water resource management, environmental sustainability, and other areas. Accurate estimation of ET_0 is a challenge in Nigeria due to the

unavailability of reliable data on the variables required for its estimation (Adesogan & Sasanya 2023). Enhanced ET_0 data using readily accessible information may guide irrigation strategies, improve water efficiency and minimise waste. This may result in higher crop yields, enhanced food security, reduced irrigation expenses for farmers, and, ultimately, greater economic sustainability and profitability. Irrigation water management is a major issue in agricultural development in Nigeria (Oluniyi & Bala 2021). Localised ET_0 models include area climate and soil variables to help farmers make irrigation choices tailored to their crops and localities. Drought significantly affects agriculture in some parts of Nigeria (Shiru *et al.* 2020). ET_0 models may pinpoint regions with elevated ET_0 levels, aiding in creating drought readiness plans, reducing crop losses, and promoting agricultural resilience.

The new models contribute to sustainable water management in Nigeria by improving the accuracy of ET_0 estimates and enabling better irrigation planning and water resource allocation. Precise evapotranspiration data may assist water managers in distributing water resources more effectively across different sectors, such as agricultural, residential consumption, and industrial requirements. Comprehending ET_0 patterns may help develop reservoir operating plans to optimise water storage and release to fulfil needs while preserving ecological balance. Integrating ET_0 into hydrological models may enhance the precision of flood predictions, facilitating prompt preparation and mitigation measures. Optimising water use in agriculture reduces water footprints, decreases environmental effects, and conserves valuable resources.

Standard statistical metrics often focus solely on overall ET_0 magnitude agreement, overlooking crucial aspects such as timing, frequency, and variability of ET_0 events. These characteristics are vital for comprehending drought dynamics, where short-term deficits and episodic droughts matter more than long-term averages. While accurate ET_0 estimation based on statistical metrics is valuable, it does not guarantee optimal performance in various hydrological applications. A model might accurately estimate observed ET_0, yet its simulations can yield different drought occurrence estimations using standard indices or depict distinct aridity patterns. This discrepancy arises from neglecting crucial ET_0 characteristics relevant to drought and aridity assessments, which were not evaluated during model development. In addition, models might perform differently when used in conjunction with other variables. Further study can be conducted to assess the performance of the models in accurately estimating drought, aridity, or other hydro-climatic events.

This study has pioneered a novel methodology for estimating ET_0 tailored for Nigeria. Its focus on Nigeria may restrict its immediate generalizability. However, developing new models that effectively estimate ET_0 using a limited set of meteorological variables significantly contributed to Nigeria's irrigation and water resources management. Moreover, the research contributes significantly to developing a methodology for constructing ET_0 models, setting a precedent for future endeavours to formulate ET_0 equations for diverse geographical regions beyond Nigeria.

5. CONCLUSION

In conclusion, this study has successfully advanced the ET_0 estimation by developing empirical models using PSO with temperature, wind speed, and relative humidity data. The comparison of these models against widely used existing ones revealed a substantial and promising improvement in performance, as evidenced by higher statistical indices, specifically KGE and Pbias. The temperature-based model, Awhari1, emerged as a standout, showing a mean KGE of 0.75 and a Pbias of 6.49%, showing a remarkable enhancement compared with established models like Ivanov. Awhari2 demonstrated an even more impressive performance, with KGE values of 0.92 and a Pbias of 5.67. These results demonstrate that the new models can estimate ET_0 in diverse climatic conditions with Nigeria with heightened accuracy and reduced uncertainty. The spatial distribution analysis of model parameters, allowing for comprehensive calibration and validation at different grid points, provides a notable novelty and addresses the insight of daily percentage bias, offering valuable implications for designing irrigation and water resource management strategies in agricultural production. Moreover, a spatial performance comparison of observed and computed daily evaporation across grid cells provides a striking visualisation of model effectiveness. The ability to address Pbias variations between observed and model values at the grid cell level demonstrates the adaptability of the developed models, fostering confidence in transferring parameter values from one region to another, even within a diverse environmental context. These findings significantly contribute to ET_0 estimation, particularly in regions with limited data availability and diverse climatic conditions.

FUNDING

The authors received no financial support for this article's research, authorship, and publication.

AVAILABILITY OF CODE

The codes used for data processing can be provided by the corresponding author at request.

CONSENT FOR PUBLICATION

All the authors consented to publish the paper.

AUTHORS CONTRIBUTION

A.P.D.: Conceptualisation, Methodology, Software, Validation, Formal analysis, Investigation, Resources, Data Curation, Writing – Original Draft, Writing – Review & Editing, Visualisation; M.H.J.: Formal analysis, Investigation, Data Curation, Writing – Original Draft, Writing – Review & Editing, Visualisation, Supervision; M.K.I.M.: Formal analysis, Investigation, Data Curation, Writing – Original Draft, Writing – Review & Editing, Visualisation, Supervision; K.B.M.: Methodology, Formal analysis; Z.M.Y.: Methodology, Software, Formal analysis, Writing – Review & Editing, Visualisation, Supervision; S.S.: Methodology, Software, Validation, Formal analysis, Investigation, Data Curation, Writing – Review & Editing, Visualisation, Supervision.

DATA AVAILABILITY STATEMENT

All relevant data are included in the paper or its Supplementary Information.

CONFLICT OF INTEREST

The authors declare there is no conflict.

REFERENCES

Adesogan, S. O. & Sasanya, B. F. 2023 Efficiency of indirect and estimated evapotranspiration methods in South Western Nigeria. *International Journal of Hydrology Science and Technology* **15** (1), 64. https://doi.org/10.1504/IJHST.2023.127895.

Ahooghalandari, M., Khiadani, M. & Jahromi, M. E. 2016 Developing equations for estimating reference evapotranspiration in Australia. *Water Resources Management* **30** (11), 3815–3828. https://doi.org/10.1007/s11269-016-1386-7.

Al-Bakri, J. T., D'Urso, G., Batchelor, C., Abukhalaf, M., Alobeiaat, A., Al-Khreisat, A. & Vallee, D. 2022 Remote sensing-based agricultural water accounting for the North Jordan Valley. *Water* **14** (8), 1198. https://doi.org/10.3390/w14081198.

Albrecht, F. 1950 Die methoden zur bestimmung der verdunstung der natürlichen erdoberfläche. *Archiv für Meteorologie, Geophysik Und Bioklimatologie, Serie B* **2**, 1–38.

Animashaun, I. M., Oguntunde, P. G., Olubanjo, O. O. & Akinwumiju, A. S. 2023 Analysis of variations and trends of temperature over Niger central hydrological area, Nigeria, 1911–2015. *Physics and Chemistry of the Earth, Parts A/B/C* **131**, 103445. https://doi.org/10.1016/j.pce.2023.103445.

Ankindawa, B. A. & Awhari, D. P. 2010 Assessing the effect of salinity on an irrigated land. *Leonardo Journal of Sciences* **1** (17), 1–8.

Araghi, A., Martinez, C. J., Olesen, J. E. & Hoogenboom, G.2022 Assessment of nine gridded temperature data for modeling of wheat production systems. *Computers and Electronics in Agriculture* **199**, 107189.

Awhari, D. P., Jamal, M. H. B., Muhammad, M. K. I. & Shahid, S. 2024 Bibliometric analysis of global climate change and agricultural production: Trends, gaps and future directions. *Irrigation and Drainage*. https://doi.org/10.1002/ird.2950.

Bai, L., Cai, J., Liu, Y., Chen, H., Zhang, B. & Huang, L. 2017 Responses of field evapotranspiration to the changes of cropping pattern and groundwater depth in large irrigation district of Yellow River basin. *Agricultural Water Management* **188**, 1–11. https://doi.org/10.1016/j.agwat.2017.03.028.

Baier, W. & Robert, G. W. 1965 Estimation of latent evaporation from simple weather observations. *Canadian Journal of Plant Science* **45**, 276–284.

Baier, W. 1971 Evaluation of latent evaporation estimates and their conversion to potential evaporation. *Canadian Journal of Plant Science* **51** (4), 255–266. https://doi.org/10.4141/cjps71-053.

Bashir, R. N., Khan, F. A., Khan, A. A., Tausif, M., Abbas, M. Z., Shahid, M. M. A. & Khan, N. 2023 Intelligent optimization of reference evapotranspiration (ET_0) for precision irrigation. *Journal of Computational Science* **69**, 102025. https://doi.org/10.1016/j.jocs.2023.102025.

Berti, A., Tardivo, G., Chiaudani, A., Rech, F. & Borin, M. 2014 Assessing reference evapotranspiration by the Hargreaves method in north-eastern Italy. *Agricultural Water Management* **140**, 20–25. https://doi.org/10.1016/j.agwat.2014.03.015.

Bodjrenou, R., Cohard, J.-M., Hector, B., Lawin, E. A., Chagnaud, G., Danso, D. K., N'tcha M'po, Y., Badou, F. & Ahamide, B. 2023 Evaluation of reanalysis estimates of precipitation, radiation, and temperature over Benin (West Africa). *Journal of Applied Meteorology and Climatology* **62** (8), 1005–1022. https://doi.org/10.1175/JAMC-D-21-0222.1.

Brockamp, B. & Wenner, H. 1963 Verdunstungsmessungen auf den Steiner see bei münster. *Deutsche Gewässerkundliche Mitteilungen* **7**, 149–154.

Dong, J., Xing, L., Cui, N., Guo, L., Liang, C., Zhao, L., Wang, Z. & Gong, D. 2024 Estimating reference crop evapotranspiration using optimized empirical methods with a novel improved Grey Wolf Algorithm in four climatic regions of China. *Agricultural Water Management* **291**, 108620. https://doi.org/10.1016/j.agwat.2023.108620.

Dooreng, J. & Pruitt, W. 1977 *Crop Water Requirements*. FAO Irrigation and Drainage Paper 24. Land and Water Development Division, FAO, Rome, p. 144.

Dorji, U., Olesen, J. E. & Seidenkrantz, M. S. 2016 Water balance in the complex mountainous terrain of Bhutan and linkages to land use. *Journal of Hydrology: Regional Studies* **7**, 55–68. https://doi.org/10.1016/j.ejrh.2016.05.001.

Droogers, P. & Allen, R. G. 2002 Estimating reference evapotranspiration under inaccurate data conditions. *Irrigation and Drainage Systems* **16** (1), 33–45. https://doi.org/10.1023/A:1015508322413.

El-Mahdy, M. E.-S., Abbas, M. S. & Sobhy, H. M. 2021 Development of mass-transfer evaporation model for Lake Nasser, Egypt. *Journal of Water and Climate Change* **12** (1), 223–237. https://doi.org/10.2166/wcc.2019.116.

Emeka, N., Ikenna, O., Okechukwu, M., Chinenye, A. & Emmanuel, E. 2021 Sensitivity of FAO Penman–Monteith reference evapotranspiration (ET_0) to climatic variables under different climate types in Nigeria. *Journal of Water and Climate Change* **12** (3), 858–878. https://doi.org/10.2166/wcc.2020.200.

FitzGerald, D. 1886 Evaporation. *Transactions of the American Society of Civil Engineers* **15** (1), 581–646. https://doi.org/10.1061/TACEAT.0000570.

Gad, A. G. 2022 Particle swarm optimization algorithm and its applications: A systematic review. *Archives of Computational Methods in Engineering* **29** (5), 2531–2561. https://doi.org/10.1007/s11831-021-09694-4.

García-Tejero, I. F., Durán-Zuazo, V. H., Muriel-Fernández, J. L. & Rodríguez-Pleguezuelo, C. R. 2011 *Water and Sustainable Agriculture*. Springer, Netherlands. https://doi.org/10.1007/978-94-007-2091-6.

Gbode, I. E., Babalola, T. E., Diro, G. T. & Intsiful, J. D. 2023 Assessment of ERA5 and ERA-interim in reproducing mean and extreme climates over West Africa. *Advances in Atmospheric Sciences* **40** (4), 570–586. https://doi.org/10.1007/s00376-022-2161-8.

Gupta, H. V. & Kling, H. 2011 On typical range, sensitivity, and normalization of mean squared error and Nash-Sutcliffe efficiency type metrics. *Water Resources Research* **47** (10), 1–3. https://doi.org/10.1029/2011WR010962.

Hamon, W. R. 1963 Computation of direct runoff amounts from storm rainfall. *International Association of Scientific Hydrology Publication* **63**, 52–62.

Hargreaves, G. H. & Samani, Z. A. 1985 Reference crop evapotranspiration from temperature. *Applied Engineering in Agriculture* **1**, 96–99.

Hernández-Bedolla, J., Solera, A., Sánchez-Quispe, S. T. & Domínguez-Sánchez, C. 2023 Comparative analysis of 12 reference evapotranspiration methods for semi-arid regions (Spain). *Journal of Water and Climate Change* **14** (9), 2954–2969. https://doi.org/10.2166/wcc.2023.448.

Huang, D., Wang, J. & Khayatnezhad, M. 2021 Estimation of actual evapotranspiration using soil moisture balance and remote sensing. *Iranian Journal of Science and Technology Transactions of Civil Engineering* **45**, 2779–2786. https://doi.org/10.1007/s40996-020-00575-7.

Islam, S., Abdullah, R. A. B., Tirth, V., Shahid, S., Algarni, S. & Hirol, H. 2020 Evaluation of mass transfer evapotranspiration models under semiarid conditions using MCDM approach. *Applied Ecology and Environmental Research* **18** (5), 6355–6375. https://doi.org/10.15666/aeer/1805_63556375.

Juneja, M. & Nagar, S. K. 2016 Particle swarm optimization algorithm and its parameters: A review. In *2016 International Conference on Control, Computing, Communication and Materials (ICCCCM)*, pp. 1–5. https://doi.org/10.1109/ICCCCM.2016.7918233.

Kharrufa, N. S. 1985 Simplified equation for evapotranspiration in arid regions. *Beiträge Zur Hydrologie, Sonderheft* **5** (1), 39–47.

Kohler, M., Vellasco, M. M. B. R. & Tanscheit, R. 2019 PSO + : A new particle swarm optimization algorithm for constrained problems. *Applied Soft Computing* **85**, 105865. https://doi.org/10.1016/j.asoc.2019.105865.

Linacre, E. T. 1977 A simple formula for estimating evaporation rates in various climates, using temperature data alone. *Agricultural Meteorology* **18** (6), 409–424. https://doi.org/10.1016/0002-1571(77)90007-3.

Mahringer, W. 1970 Verdunstungsstudien am neusiedler see. *Archiv für Meteorologie, Geophysik Und Bioklimatologie, Serie B* **18**, 1–20.

Meyer, A. 1926 Über einige zusammenhänge zwischen klima und boden in Europa. ETH, Zurich.

Muhammad, M. K. I., Shahid, S., Hamed, M. M., Harun, S., Ismail, T. & Wang, X. 2022 Development of a temperature-based model using machine learning algorithms for the projection of evapotranspiration of Peninsular Malaysia. *Water* **14** (18), 2858. https://doi.org/10.3390/w14182858.

Nikolaou, G., Neocleous, D., Christou, A., Kitta, E. & Katsoulas, N. 2020 Implementing sustainable irrigation in water-scarce regions under the impact of climate change. *Agronomy* **10** (8), 1120. https://doi.org/10.3390/agronomy10081120.

Oguntunde, P. G., Abiodun, B. J. & Lischeid, G. 2011 Rainfall trends in Nigeria, 1901–2000. *Journal of Hydrology* **411** (3–4), 207–218. https://doi.org/10.1016/j.jhydrol.2011.09.037.

Oloyede, M. O., Williams, A. B., Ode, G. O. & Benson, N. U. 2022 Coastal vulnerability assessment: A case study of the Nigerian coastline. *Sustainability* **14** (4), 2097. https://doi.org/10.3390/su14042097.

Oluniyi, E. O. & Bala, M. S. 2021 Irrigation management in Nigeria: Lessons from the Kano River irrigation scheme. *Irrigation and Drainage* **70** (3), 517–523. https://doi.org/10.1002/ird.2586.

Papadakis, J. 1965 *Crop Ecologic Survey in Relation to Agricultural Development of Western Pakistan*. Draft Report. FAO: Rome, Italy.

Penman, H. L. 1948 Natural evaporation from open water, bare soil and grass. *Proceedings of the Royal Society of London. Series A. Mathematical and Physical Sciences* **193**, 120–145.

Quagraine, K. A., Nkrumah, F., Klein, C., Klutse, N. A. B. & Quagraine, K. T. 2020 West African summer monsoon precipitation variability as represented by reanalysis datasets. *Climate* **8** (10), 111. https://doi.org/10.3390/cli8100111.

Ravazzani, G., Corbari, C., Morella, S., Gianoli, P. & Mancini, M. 2012 Modified Hargreaves-Samani equation for the assessment of reference evapotranspiration in Alpine river basins. *Journal of Irrigation and Drainage Engineering* **138** (7), 592–599. https://doi.org/10.1061/(ASCE)IR.1943-4774.0000453.

Rohwer, C. 1931 *Evaporation From Free Water Surfaces*. United States Department of Agriculture, Economic Research Service, Washington, DC. DOI: 10.22004/ag.econ.163103.

Romanenko, V. 1961 Computation of the autumn soil moisture using a universal relationship for a large area. *Proceedings of Ukrainian Hydrometeorological Research Institute* **3**, 12–25.

Roy, D. K., Lal, A., Sarker, K. K., Saha, K. K. & Datta, B. 2021 Optimization algorithms as training approaches for prediction of reference evapotranspiration using adaptive neuro fuzzy inference system. *Agricultural Water Management* **255**, 107003. https://doi.org/10.1016/j.agwat.2021.107003.

Schendel, U. 1967 Vegetationswasserverbrauch und-wasserbedarf. *Habilitation, Kiel* **137**, 1.

Shiri, J. 2017 Evaluation of FAO56-PM, empirical, semi-empirical and gene expression programming approaches for estimating daily reference evapotranspiration in hyper-arid regions of Iran. *Agricultural Water Management* **188**, 101–114. https://doi.org/10.1016/j.agwat.2017.04.009.

Shiru, M. S., Shahid, S., Dewan, A., Chung, E. S., Alias, N., Ahmed, K. & Hassan, Q. K. 2020 Projection of meteorological droughts in Nigeria during growing seasons under climate change scenarios. *Scientific Reports* **10** (1). https://doi.org/10.1038/s41598-020-67146-8.

Singh, V. P. & Xu, C.-Y. 1997 Evaluation and generalization of 13 mass-transfer equations for determining free water evaporation. *Hydrological Processes* 11, 311–323. https://doi.org/10.1002/(sici)1099-1085(19970315)11:3<311::aid-hyp446>3.0.co;2-y.

Steinkopf, J. & Engelbrecht, F. 2022 Verification of ERA5 and ERA-interim precipitation over Africa at intra-annual and interannual timescales. *Atmospheric Research* **280**, 106427. https://doi.org/10.1016/j.atmosres.2022.106427.

Szasz, G. 1973 A potenciális párolgás meghatározásának új módszere. *Hidrológiai Közlöny* **10**, 435–442.

Tabari, H. & Talaee, P. H. 2011 Local calibration of the Hargreaves and Priestley-Taylor equations for estimating reference evapotranspiration in arid and cold climates of Iran based on the Penman-Monteith model. *Journal of Hydrologic Engineering* **16** (10), 837–845. https://doi.org/10.1061/(ASCE)HE.1943-5584.0000366.

Trabert, W. 1896 Neue beobachtungen über verdampfungsgeschwindigkeiten. *Meteorologische Zeitschrift* **13**, 261–263.

Trajkovic, S. 2007 Hargreaves versus Penman-Monteith under humid conditions. *Journal of Irrigation and Drainage Engineering* **133** (1), 38–42. https://doi.org/10.1061/(ASCE)0733-9437(2007)133:1(38).

Wang, D., Tan, D. & Liu, L. 2018 Particle swarm optimization algorithm: An overview. *Soft Computing* **22** (2), 387–408. https://doi.org/10.1007/s00500-016-2474-6.

World Meteorological Organization (WMO), Harbeck, G. E., Nordenson, T. J., Omar, M. H. & Uryvaev, V. A. 1966 *Commission for Instruments and Methods of Observation (CIMO). Measurement and Estimation of Evaporation and Evapotranspiration: Report of a Working Group on Evaporation Measurement of the Commission for Instruments and Methods of Observation*. WMO. Available at: https://library.wmo.int/records/item/59800-measurement-and-estimation-of-evaporation-and-evapotranspiration.

Wu, Z., Li, Q., Chen, Q., Zhou, Z. & Chen, Y. 2023 Comparison and evaluation of evapotranspiration estimations by different approaches in the Yellow River Basin. *Journal of Water and Climate Change* **14** (8), 2719–2735. https://doi.org/10.2166/wcc.2023.072.

Xu, H.-Q., Gu, S., Fan, Y.-C., Li, X.-S., Zhao, Y.-F., Zhao, J. & Wang, J.-J. 2023 A strategy learning framework for particle swarm optimization algorithm. *Information Sciences* **619**, 126–152. https://doi.org/10.1016/j.ins.2022.10.069.

Zaman, A., Zaman, P. & Maitra, S. 2017 Water resource development and management for agricultural sustainability. *Journal of Applied and Advanced Research* 73–77. https://doi.org/10.21839/jaar.2017.v2i2.61.

Zhang, Y. & Kong, X. 2023 A particle swarm optimization algorithm with empirical balance strategy. *Chaos, Solitons & Fractals: X* **10**, 100089. https://doi.org/10.1016/j.csfx.2022.100089.

First received 12 March 2024; accepted in revised form 15 May 2024. Available online 25 June 2024